

Bypassing particle-mediated adverse injection reactions through shape modification and erythrocyte ‘hitch-hiking’

Peter P. Wibroe,¹ Aaron C. Anselmo,² Per H. Nilsson,³ Vivek Gupta,⁴ Rudolf Urbanics,⁵ Janos Szebeni,⁵ A. Christy Hunter,⁶ Samir Mitragotri,² Tom Eirik Mollnes,^{3,7,8} Seyed Moein Moghimi^{1,9,10*}

¹Nanomedicine Laboratory, Centre for Pharmaceutical Nanotechnology and Nanotoxicology, Department of Pharmacy, Faculty of Health and Medical Sciences, University of Copenhagen, Universitetsparken 2, DK-2100 Copenhagen Ø, Denmark

²University of California at Santa Barbara, Department of Chemical Engineering and Center for Bioengineering, Santa Barbara, CA 93106, USA

³Department of Immunology, Oslo University Hospital Rikshospitalet, and K.G. Jebsen IRC, University of Oslo, 0372 Oslo, Norway

⁴School of Pharmacy, Keck Graduate Institute, 535 Watson Drive, Claremont, CA 91711, USA

⁵Nanomedicine Research and Education Center, Semmelweis University, Budapest & SeroScience Ltd, Budapest, Hungary

⁶Leicester School of Pharmacy, De Montfort University, The Gateway, Leicester LE1 9BH, UK

⁷Reserach Laboratory, Nordland Hospital, 8092 Bodø, and K.G. Jebsen TREC, University of Tromsø, 9037 Tromsø, Norway

⁸Centre of Molecular Inflammation Research, Norwegian University of Science and Technology, 7491 Trondheim, Norway

⁹Nano-Science Center, University of Copenhagen, Universitetsparken 5, DK-2100 Copenhagen Ø, Denmark

¹⁰School of Medicine, Pharmacy and Health, Durham University, Queen’s Campus, Stockton-on-Tees TS17 6BH, United Kingdom

*Corresponding author: School of Medicine, Pharmacy and Health, Durham University, Queen’s Campus, Stockton-on-Tees TS17 6BH; moein.moghimi@gmail.com; seyed.m.moghimi@durham.ac.uk

Intravenously injected nanopharmaceuticals induce adverse cardiopulmonary reactions in sensitive human subjects and these reactions are reproducible in pigs. The underlying mechanisms are poorly understood, but a role for both the complement system and reactive macrophages has been implicated. Here we show the dominance and importance of early pulmonary intravascular macrophage clearance kinetics in adverse particle-mediated cardiopulmonary distress in pigs and irrespective of complement activation. Delaying particle recognition by macrophages within the first few minutes of injection overcome adverse reactions in pigs. This was achieved by two independent approaches: (i) changing particle geometry from a spherical shape (which trigger cardiopulmonary distress) to either rod- or disk-shape morphology and (ii) by physically adhering spheres to the surface of erythrocytes. These approaches bypasses particle surface engineering approaches to prevent robust macrophage recognition as well as the use of immunological or pharmacological modulators to reduce/overcome nanomedicine related adverse cardiopulmonary distress.

Intravenous administration of liposomal and polymeric nanopharmaceuticals is known to incite autonomic, muco-cutaneous and cardiopulmonary reactions in some human patients¹⁻⁵. Symptoms include fever, chills, wheezing, facial swelling, flushing, rash, coughing, shortness of breath, tachypnea, hypertension/hypotension and chest and back pain. These symptoms range from light to severe and are not initiated by pre-existing allergen-reactive immunoglobulins (e.g., IgE type antibodies)^{4,5}.

The underlying mechanism(s) behind intravenous injection reactions to nanopharmaceuticals is poorly understood. Inadvertent activation of the complement system, which is the first line of the body's defence against foreign intruders, has been suggested to be a causal factor^{4,5}. Liberated complement anaphylatoxins C3a and C5a can modulate the function of responder immune cells such as mast cells, neutrophils, basophils, eosinophils and macrophages causing rapid release of a secondary mediators that negatively affect the cardiovascular system^{4,6,7}. Nanopharmaceutical-mediated cardiopulmonary responses in sensitive human subjects are reproducible in pigs, which include a massive increase in pulmonary arterial pressure (PAP) and decline in the systemic arterial pressure (SAP)⁸. Moreover, earlier studies have shown a role for

complement activation and particularly C5a in the development of cardiopulmonary distress in pigs⁹.

Unlike humans, pigs (and sheep) have resident pulmonary intravascular macrophages (PIMs)^{10,11}. PIMs instantaneously ingest intravenously injected particles and subsequently release large quantities of thromboxane A2 (TxA2), prostaglandins and prostacyclins that correlate with periods of peak vasoconstriction, bronchoconstriction and pulmonary hypertension¹¹. Furthermore, earlier studies have demonstrated that newborn lambs prior to developing PIMs show no changes in PAP after particle injection¹². Within two weeks of birth, lambs develop a population of PIMs, which is accompanied by increased lung accumulation of injected particles with a concomitant increase in PAP and TxA2 production¹². Collectively, these observations suggest that PIMs on robust phagocytosis may induce anaphylaxis. Complement anaphylatoxins may further modulate the function of PIMs as well as other immune cells and aggravate cardiopulmonary reactions¹³. For instance, C5a can synergistically enhance Toll-like receptor-induced production of pro-inflammatory cytokines and further promote TxA2 release¹⁴. In line with the role of macrophages in anaphylaxis, a recent hypothesis has suggested that human subjects who are sensitive to nanopharmaceutical administration presumably have a subset of highly responsive resident macrophages in pulmonary circulation¹⁵. Indeed, there are suggestions of induction of pulmonary macrophages in subjects with liver abnormalities and other hepato-pulmonary diseases^{10,11,16,17}.

Accordingly, methods to circumvent robust macrophage association and internalization may present an attractive mean to limit nanopharmaceutical-mediated cardiopulmonary distress. Surface modification of nanoparticles with poly(ethylene glycol) (PEG) is a well-established strategy to combat rapid macrophage interception¹⁸.

Unfortunately, acute adverse injection reactions with PEGylated liposomes and nanoparticles still persist in some human subjects as well as in pigs^{4,5,8,9,18-20}. Indeed, PEGylated particles can not only trigger complement activation¹⁸⁻²², but they are also prone to rapid recognition by a subset of monocyte/macrophage populations independent of opsonization processes^{23,24}.

If macrophages in the pulmonary circulation play an important role in anaphylaxis, then it is imperative to prevent particle-macrophage interaction within the first few minutes of injection where reactions typically develop. Recently, it was shown that particle shape could be a pivotal parameter in combating recognition by macrophages²⁵⁻²⁸. Parallel to these attempts, particle ‘hitch-hiking’ on erythrocytes also afford protection to robust particle ingestion by macrophages in contact with the blood^{29,30}. Here, we employ these strategies, which may be applicable to different clinical scenarios and show that by leveraging both particle shape modifications and erythrocyte ‘hitch-hiking’, dampening or overcoming particle-mediated adverse cardiopulmonary reactions on bolus injection occurs.

Particle shape. We utilized carboxylated polystyrene particles of spherical, prolate ellipsoidal (rods), and oblate ellipsoidal (disks) shapes bearing a comparable range of Gaussian curvatures (**Figure 1**). We assessed propensity of these particles to 1) incite complement in pig³¹ and human blood^{21,22}, and 2) induce haemodynamic disturbances *in vivo* in the pig model^{8,9}.

The results in **Figure 2a&b** show the effect of the particle shape on time-dependent complement activation in the pig blood. Complement activation was monitored through measurements of sC5b-9 (a nonlytic soluble marker of the terminal pathway of the complement system and a sensitive measure of the activation of the

whole complement cascade) and anaphylatoxin C5a^{21,22,32}, relative to a zymosan (an established potent activator of the complement system) response. Absolute values of complement activation products are given in **Supplementary Figure S1**. We compared complement activation at an equivalent surface area for each particle type (~14,500 mm²/mL of blood). Spheres (500 nm) did not incite complement within the first 5 min of incubation. At later time-points some complement activation occurred, which was statistically significant (**Figure 2a&b**). Similar to spheres, rods and disks did not induce complement activation within the first 5 min, but later complement activation was robust and more profound than spheres. Since stretching spheres at high temperature generated rods and disks, these conditions may have created complement-activating surface domains due to altered polystyrene re-packaging and configuration. Indeed, alterations in polymer configuration can incite complement through different pathways.³³

We further observed a similar time-dependent complement activation (through measurements of C3bc, C3a, C5a and sC5b-9) profile by the particles in the human blood, but unlike pig blood complement activation by all particles were comparable at late time points (**Supplementary Figure S2**). The reasons for these differences are not clear, but may be related to differences in protein corona on particles in pig and human blood and subsequent complement activation by adsorbed proteins. Since these particles did not trigger complement activation instantaneously in porcine and human blood, we next assessed haemodynamic responses on particle injection in pigs.

Particles were injected intravenously at an equivalent surface area (~114,300 mm²/20 kg body weight) into pigs in a total volume of 5-10 mL over 30s to 2 min and they showed a different trend in cardiopulmonary responses. Immediately on injection, spheres elevated PAP with a concomitant decline in SAP (**Figure 2c & d**).

Haemodynamic disturbances, however, were restored within 5 min of injection. These haemodynamic responses were comparable to a 0.5 mg/kg zymosan dose (**Supplementary Figure S3**), but unlike spheres, zymosan is a potent and an instantaneous activator of the complement system^{8,21,22}. However, administration of the prostaglandin inhibitor indomethacin attenuated zymosan- and sphere-induced rises in PAP (**Supplementary Figure S3**). In contrast to spheres, neither rods nor disks induced notable cardiopulmonary disturbances and minute PAP rises were peaked slightly later (**Figure 2c**). Afterwards, PAP rises were returned to background level by 10 min and there were no further elevation at 20 min post injection, despite the fact that rods and disks induced notable complement activation in pig blood from 10 min onward. The shape-dependent cardiopulmonary distress differences in pigs were also reflected by the ability of the spheres to elevate thromboxane B2 (TxB₂), an inactive metabolite of the vasoconstrictor TxA₂ released predominantly by macrophages, at the peak level of PAP³⁴ (**Figure 2e**).

These observations indicate that perturbations in haemodynamic parameters may be complement-independent and could be related to kinetics of particle clearance by PIMs. Accordingly, robust particle removal from the blood (as in spheres or zymosan particles) may initiate cardiopulmonary disturbances. Next, we used rhodamine-labelled particles to compare their clearance rates from the porcine circulation on intravenous injection at an equivalent particle number (1.5×10^{11} particles/20 kg body weight). The results in **Figure 3** show that both rods and disks circulate longer than spheres. Notably, a large proportion of spheres are cleared from the blood within 2 min of injection compared with rods and disks, which coincide with peak PAP and TxB₂ levels. These findings corroborate with the suggestion that immediate and robust particle phagocytosis by PIMs may largely control the magnitude

of cardiopulmonary responses¹⁵. Thus, to further show a role for PIMs in cardiopulmonary distress responses, we performed a second set of experiments in pigs where the majority of PIMs were depleted by prior administration of clodronate-encapsulated liposomes³⁵ (**Figure 4**). Indeed, on PIM depletion, carboxylated sphere (injected at 1.5×10^{11} particle/20 kg body weight)-mediated PAP and TxB₂ rises were dramatically dampened. Furthermore, similar observations were obtained on injection of other particle types such as sulfated polystyrene particles (500 nm in size and at 1.5×10^{11} particle/20 kg body weight) and PEGylated liposomes (200 nm in size and 10 mg total lipid/20 kg body weight) following PIM depletion (**Figure 4**).

We further used radiolabelled particles to investigate their clearance kinetics and biodistribution in the mouse model, which physiologically do not possess PIMs. The results showed similar particle shape-dependent blood clearance profile as in pigs (**Supplementary Figure S4**). After 10 min of injection the blood concentration of all three particle types were similar and corresponded to <10% of the administered dose. Biodistribution analysis confirmed eventual particle confinement to the murine macrophage-rich organs (liver and spleen) (**Supplementary Figure S4**) and irrespective of particle shape.

The intravenous route of administration rapidly exposes particles to the lung capillaries³⁶, thereby placing the particles in direct and immediate contact with pulmonary macrophages in pigs. The dimensions of rods and disks used in this study, however, are not sufficiently large (i.e., they are not in micron-range dimensions) to allow conditions of shear flow and vascular anatomy to modulate particle dynamics and orientation in the systemic circulation^{37,38}. Therefore, it is highly plausible that rods and disks of current dimensions assume random orientation in the blood, where an end-on (for rods) or edge-on (for disks) approach (high curvature domains) may overcome

rapid sensing and recognition by macrophages, thereby explaining their slower clearance rate from the blood compared with spheres. Accordingly, only a fraction of rods and disks are sensed by PIMs at a typical blood circulation round, which correlate with low PAP rises.

In agreement with this notion, J774 macrophages under static conditions also showed the trend of significantly faster uptake of spheres compared with rods and disks in the first minute of mixing, followed by comparable uptake levels at all later time points where particles have settled and macrophages have the opportunity to engulf particles of different orientations (**Supplementary Figure S5**). The slower clearance rate of rods and disks by PIMs may have therefore triggered a desensitization process³⁹, and consequentially prevented the release of secondary mediators responsible for initiating cardiopulmonary distress. Clinical studies have shown that slowing the infusion rate of nanomedicines decreases the magnitude of adverse reactions in sensitive human subjects^{4,5}. A plausible explanation for this phenomenon is the reduced rate of particle presentation to the putative induced pulmonary macrophages in sensitive subjects¹⁵. Finally, our results may also explain why administration of a recently designed artificial phospholipid disk-shaped particle did not incite adverse cardiopulmonary distress in pigs, as they may have been cleared from the blood at a slow rate by PIMs⁴⁰.

Particle ‘hitch-hiking’ on erythrocytes. Earlier, it was shown that adsorption of particles of different sizes (e.g., 110-1100 nm) and surface functionalities (e.g., carboxyl, amine, aldehyde and polyethylene amine) to erythrocytes occur, which subsequently improve their circulation times^{29,30}. Since PIMs played a central role in injection reactions to particles, we reasoned that a transient delay in extraction of

spherical particles by macrophages through erythrocyte ‘hitch-hiking’ may dampen haemodynamic disturbances. To test this hypothesis we first used larger (750 nm) carboxylated polystyrene spheres to induce more efficient complement activation^{18,21}. The results in **Figure 4a-d** show association of carboxylated spheres to both human and pig erythrocytes in the absence of plasma, which remain bound upon plasma restoration. The results further shows that spheres in free form or attached to erythrocytes induce comparable complement activation (**Figure 4e**). On intravenous injection, erythrocyte ‘hitch-hiked’ particles did not elevate PAP considerably, but unbound particles induced a substantial rise in PAP (**Figure 4f**). The low PAP responses with ‘hitch-hiked’ systems may have been caused by the presence of the 30% unbound particles to erythrocytes (**Figure 4c**). These haemodynamic observations were also reproducible with poor complement activating 500 nm spheres bound to erythrocytes (**Supplementary Figure S6**), which additionally highlight detection of increased thromboxane levels on administration of unbound particles as opposed to ‘hitch-hiked’ particles. Taken together, these results imply that erythrocyte ‘hitch-hiking’ decreases particle-mediated cardiopulmonary distress by avoiding early interactions with macrophages irrespective of complement activation.

Finally, we suggest that erythrocyte ‘hitch-hiking’ may serve an alternative approach for alleviating adverse injection reaction to currently available spherically-shaped polymeric drug carriers such as poly(cyanoacrylate) and poly(DL-lactide-co-glycolide) and their derivative thereof^{1,41}. Indeed, these particles can adhere to erythrocytes in the absence of plasma and remain bound on plasma restoration³⁰.

Conclusions. We showed for a set of different-shaped polystyrene particles how the kinetics of macrophage clearance dictates the extent of cardiopulmonary responses

irrespective of complement activation. Robust particle interaction with macrophage appears to be an important factor in the development of adverse injection reactions, which is presumably regulated by the type of macrophage receptor(s) and associated signalling. Although, the identity of these receptors remains unknown, we dampened cardiopulmonary distress in pigs by two independent approaches that attenuated rapid particle-macrophage interactions. The first approach was to use particles displaying rod or disk morphologies with dimensions below 500 nm. The second approach resolved adverse injection reaction to spherical particles through their prior adherence to erythrocytes. These strategies avoided the use of immunological or pharmacological manipulations^{42,43} and did not require prior particle surface modification with polymers^{33,44,45}. These ‘simple-by-design’ approaches may be extended to PRINT technology (Particle Replication in Non-wetting Templates)⁴⁶ for identification of other geometries and particle dimensions for overcoming injection-related reactions. Even with spherically shaped particles, erythrocyte “hitch-hiking” may provide a viable clinical solution for nanomedicine administration and salvage the use of currently available polymeric-based drug carriers for different therapeutic interventions. Finally, we suggest that PIMs act as ballerinas in particle-mediated injection reactions, while the exact role of complement needs to be explored in detail. Although inadvertent complement activation may still play a role in injection reactions, our observations, however, suggest that *in vitro* complement assessment alone may not be a sufficiently sensitive approach to predict adverse injection reactions, and for preselecting patients for safe administration of nanopharmaceuticals.

Methods

Preparation and characterization of particles

Plain carboxylated polystyrene particles of 200, 500 and 750 nm and sulfated polystyrene particles (500 nm) were purchased from Polysciences Inc. (Warrington, PA). For some studies FITC- or rhodamine-labelled carboxylated polystyrene particles were used. The 200 nm particles were stretched into rods and disks either by a one-dimensional or two-dimensional film stretching method, respectively, as previously described²⁷. Briefly, 10^{13} polystyrene spheres were first embedded into a hot water soluble polyvinyl alcohol film (10% w/v in water) with 2% (w/v) glycerol. Films were then mounted and mechanically stretched in either one or two dimensions in oil at 120°C. Films were then dissolved in 70°C water for 2 hours and then centrifuged at 8,000 g to isolate the particles. Particle suspensions were centrifuged in water 10 more times and finally passed through a 170 µm filter. Scanning electron micrographs were taken on an FEI XL40 and imaged at 5-10 kV acceleration voltage at 5 mm working distance.

PEGylated liposomes (100 and 200 nm, respectively) resembling Doxil® in lipid composition and doxorubicin content were prepared as described before³². Size analysis was performed by Nanoparticle Tracking Analysis following sample dilution ($\times 10^6$) with 10 mM NaCl and monitored with an LM20 NanoSight mounted with a blue (405 nm) laser (Malvern Instruments, UK) using the Nanosight 2.3 software for data analysis³².

In vitro complement activation in whole blood

For activation of the complement system, blood was drawn from healthy human subjects according to local approved protocols and individual consent into blood tubes containing the anticoagulant lepirudin (Refludan®, Hoechst, Frankfurt am main, Germany), which does not affect complement system⁴⁷. Pig blood was also collected in lepirudin blood tubes. Measurements on human whole blood (WB) were based on three individual donors. Measurements on pig WB were done in three different experiments using blood from a healthy pig. Particle concentration was normalized to yield constant exposed surface area. Briefly, 20 µL particles, PBS or zymosan (0.2 mg/mL) were added to WB corresponding to a volume of ~80 µL plasma (i.e 160 µL human WB and 120 µL Pig WB) and incubated at 37°C for a range of time points (1-30 min) followed by dilution in cold diluent containing EDTA to stop complement activation. After centrifugation, human C3bc and sC5b-9 was quantified by ELISA as described elsewhere⁴⁸. Pig sC5b-9 determination was done as described earlier³¹. Human and pig C5a was quantified using commercial available kits (Hycult, Uden, the Netherlands). For particles bound to erythrocytes, the blood was pretreated as stated below.

Interaction between C3a and particles

In addition to the complement markers above, C3a was also included to assess complement activation. However, due to a reduced level of measured C3a in plasma when particles were present, a potential interaction between C3a and particles was investigated. Purified human C3a (Hycult, Uden, The Netherlands) was mixed with a pool of human EDTA-treated plasma from 9 donors, reaching final C3a concentrations of 0-5400 ng/mL. This concentration range was selected to mimic the concentrations reached in zymosan-induced *in vitro* complement responses. Accordingly, the three particle shapes were introduced in amounts mimicking the incubations for *in vitro* complement activation. After 30 min incubation at 37°C, particles were pelleted and

the concentration of C3a in the supernatant was measured by ELISA (Hycult, Uden, the Netherlands) and compared with plasma samples incubated without particles.

Haemodynamic measurements in pigs

In vivo studies were performed on Yorkshire pigs (23-27 kg). This method has previously been fully detailed and validated, and approved by Semmelweis University Animal Subject Review Committee^{8,9,42}. Briefly, each pig was randomly selected and initially sedated with 40 mg/kg ketamine and then anesthetized with sodium pentobarbital (25-150 mg/h). A catheter was advanced into the right jugular vein and into the pulmonary artery for measurement of PAP and SAP. A second catheter was placed through the right femoral artery into the distal aorta, measuring systemic arterial pressure. Electrocardiogram and respiratory output was also continuously recorded and blood samples were drawn through the left jugular vein before and following particle injection to monitor blood markers. For particles bound to erythrocytes, blood samples were initially drawn into lepirudin tubes and used for erythrocyte isolation. Particles were administered through the left jugular vein in a total volume of 5-10 mL in injection saline. For treatment with indomethacin, PBS was slowly added to a solution of 6.5 mg/mL in ethanol, to reach a final indomethacin concentration of 2.6 mg/mL in 40% ethanol. A total dose of 1 mg/kg was slowly administered to the pigs 10-15 min before particle injection. In some experiments, particles were injected 24 h after PIM depletion. The latter was achieved with 4 intravenous infusions of clodronate-encapsulated multi-lamellar egg phosphatidylcholine/cholesterol (mole ratio 7:3) liposomes of 800-1700 nm range (corresponding to 1.0 g clodronate/10 kg body weight) once every 12 h³⁵. Control animals received an equal volume of empty liposomes. Fifteen random biopsy lung specimens per animal (n = 2 pigs per group) were selected for assessment of PIMs stained by Monastral blue (injected intravenously at a dose of 5mg/kg in saline 1 h before particle administration)³⁵. Slides, after fixation in 10% buffered formalin and subsequent dehydration and paraffin embedding were sectioned into 4-5 μ M thickness and then de-paraffinized, rehydrated and stained with eosin. Finally, slides were analysed for the number of positive PIM cells per high-powered field.

Thromboxane B2 was measured from the extracted blood plasma samples using a commercial thromboxane B2 Express EIA kit (Cayman Chemical, Ann Arbor, MI).

Attachment and characterization of particles to erythrocytes

Freshly drawn WB samples were centrifuged at 1,200 g for 7 min to pellet cells. Plasma was removed and stored for later use, and buffy coat was discarded. Erythrocytes were then washed in PBS 3 times. No haemolysis was observed during the handling. The final erythrocyte number was counted (Tali Image cytometer, Invitrogen USA) and mixed with particles dispersed in PBS in an erythrocyte:particle ratio of ~2:1 which was found to be optimal, and incubated 37°C for 30 min to allow particle adhesion. Lepirudin-anticoagulated plasma was then added enabling complement activation to occur, following the procedure described above. For preparations with unbound particles, erythrocytes were first incubated in presence of PBS, then reconstituted with plasma, and finally mixed with particles before complement activation. All samples were thereby treated identically, with the exception of the time of particle addition. When particles were absent, PBS was used to achieve constant volume. Samples with bound particles also contained some particles that were free. Thus, samples and injections with “bound” particles contained the same amount

of particles than “unbound” particles, although not all of them were physically bound to cells.

Characterization of the interaction between particles and erythrocytes were made on samples after activation, and inhibition of the complement system. For scanning electron microscopy, samples were diluted with 4% formaldehyde, and left at room temperature overnight. Thereafter a small volume was left drying on a silicon wafer and gently washed with water. After complete evaporation, a 20 nm gold layer was applied (Leica EM SCD005), and monitored using a JSM-6320F scanning electron microscope at 10 kV.

For FACS characterization, reacted complement samples were diluted in PBS to a total erythrocyte dilution of 10^4 and monitored on a BD FACSAArray flow cytometer with flow rate of 0.5 $\mu\text{L/s}$ and side scatter threshold of 3,000.

For light microscopy, samples were placed between two cover slips, and monitored on a Leica AF6000LX microscope using a 63x and 100x oil immersion objective (NA. 1.46) with a 1.6 magnification in DIC mode. Two filters (Ex BP 475/40 nm and Em BP 530/50 nm) were used to detect FITC-labelled spheres, and a background subtraction was made on all images to reduce dust-induced noise.

In vivo circulation and biodistribution studies

The blood clearance of rhodamine-labelled particles (spheres, rods and disks) was monitored after a single intravenous injection (1.5×10^{11} particles/25kg body weight) into pigs (n=2). At selected time points blood samples were removed and analysed for the presence of particles. The blood concentration of particles was estimated from blood samples containing known quantities of labelled particles.

In some experiments, spheres, rods and disks were radiolabelled with ^3H -oleic acid (Moravek Biochemicals) for biodistribution studies in mice. Briefly, 20% w/v particle suspension in water was added to a solution containing 100 μL [^3H]-oleic acid, 100 μL ethanol, and 25 μL tetrahydrofuran for 30 min with constant rotation. Particles were washed ten times at 15,000 g for 30 min *via* centrifugation to remove unincorporated tritium and re-suspended in saline prior to injection. For circulation and biodistribution studies, 5×10^9 radiolabeled particles were injected *via* tail vein into randomly grouped healthy female BALB/c mice (18-20 g). At specified time points, blood was drawn and mice were sacrificed *via* CO_2 overdose. Known weights of blood, liver, spleen, kidney, heart, lungs, brain, and skin were harvested and dissolved overnight at 60 $^\circ\text{C}$ in 5 mL of Solvable (Perkin Elmer). The next day, Ultima Gold (Perkin Elmer) was added to dissolved organ samples and [^3H] content was measured using a TriCarb 2100TR scintillation counter. All mouse protocols were approved by the Institutional Animal Care and Use Committee (IACUC) at the University of California, Santa Barbara, CA).

In vitro macrophage uptake

Radiolabelled particles of different shapes were prepared as described above. J774 macrophages were cultured in standard cell culture conditions (37 $^\circ\text{C}$ in 5% CO_2) in high glucose DMEM (ATCC), 10% FBS, and 1% penicillin/streptomycin. 1.5×10^4 J774 cells per well were seeded for 24 h in a 96-well plate. Prior to the experiment, particles were resuspended in DMEM containing 20% (v/v) fresh BALB/c serum, at 0.1 mg/mL and introduced to plated J774 cells following removal of DMEM containing FBS and penicillin/streptomycin and 3 washes with PBS. At specified time points, particle solutions were removed from cells, and cells were washed 3x with PBS to

remove unbound or non-internalized particles. Cells were immediately incubated at 60°C for 1 h in 5 mL of Solvable and then analyzed (as described above) for [³H] content.

Acknowledgements

SMM acknowledges financial support by the Danish Agency for Science, Technology and Innovation (Det Strategiske Forskningsråd), reference 09-065746. Financial support for the complement studies was obtained from the European Community's Seventh Framework Programme under grant agreement number 602699 (DIREKT). We acknowledge Nader Payemi (University of Copenhagen) in assisting with scanning electron microscopy studies and Hycult Biotech for providing the pig C5a ELISA kit.

Authors Contribution

PPW and SMM conceived the idea. PPW performed complement activation studies in human blood and characterized particle-erythrocyte interactions. PPW and RU contributed to *in vivo* porcine studies and TxB2 measurements. SM and ACA designed particles and macrophage and biodistribution studies. ACA synthesized and characterized polystyrene particles, conducted *in vivo* circulation and biodistribution studies in mice as well as *in vitro* uptake studies in J774 cells. VG conducted *in vivo* circulation and biodistribution studies in mice. PN performed complement activation studies in pig blood. All authors discussed and analyzed data. PPW and SMM wrote the paper with contributions from all co-authors.

Additional information

Supplementary information is available in the online version of the paper. Correspondence and requests for materials should be addressed to SMM.

Competing interests. The authors declare no competing financial interest.

References

- 1 Kattan, J. *et al.* Phase I clinical trial and pharmacokinetic evaluation of doxorubicin carried by polyisohexylcyanoacrylate nanoparticles. *Invest. New Drugs* **10**, 191-199 (1992).
- 2 Laing, R. B., Milne, L. J., Leen, C. L., Malcolm, G. P. & Steers, A. J. Anaphylactic reactions to liposomal amphotericin. *Lancet* **344**, 682 (1994).
- 3 Uziely, B. *et al.* Liposomal doxorubicin: antitumor activity and unique toxicities during two complementary phase I studies. *J. Clin. Oncol.* **13**, 1777-1785 (1995).
- 4 Moghimi, S. M., Wibroe, P. P., Helvig, S. Y., Farhangrazi, Z. S. & Hunter, A. C. Genomic perspectives in inter-individual adverse responses following nanomedicine administration: The way forward. *Adv. Drug Deliver. Rev.* **64**, 1385-1393 (2012).
- 5 Szebeni, J. Complement activation-related pseudoallergy: a stress reaction in blood triggered by nanomedicines and biologicals. *Mol. Immunol.* **61**, 163-173, (2014).
- 6 Kastl, S. P. *et al.* In human macrophages the complement component C5a induces the expression of oncostatin M via AP-1 activation. *Arterioscler. Thromb. Vasc. Biol.* **28**, 498-503 (2008).
- 7 Woodruff, T. M., Nandakumar, K. S. & Tedesco, F. Inhibiting the C5-C5a receptor axis. *Mol. Immunol* **48**, 1631-1642 (2011).
- 8 Szebeni, J. *et al.* A porcine model of complement-mediated infusion reactions to drug carrier nanosystems and other medicines. *Adv. Drug Deliv. Rev.* **64**, 1706-1716 (2012).
- 9 Szebeni, J. *et al.* Complement activation-related cardiac anaphylaxis in pigs: role of C5a anaphylatoxin and adenosine in liposome-induced abnormalities in ECG and heart function. *Am. J. Physiol. Heart Circ. Physiol.* **290**, H1050-1058 (2006).
- 10 Warner, A. E. Pulmonary intravascular macrophages. Role in acute lung injury. *Clin. Chest Med.* **17**, 125-135 (1996).
- 11 Schneberger, D., Aharonson-Raz, K. & Singh, B. Pulmonary intravascular macrophages and lung health: what are we missing? *Am. J. Physiol. Lung Cell Mol. Physiol.* **302**, L498-503 (2012).
- 12 Longworth, K. E., Westgate, A. M., Grady, M. K., Westcott, J. Y. & Staub, N. C. Development of pulmonary intravascular macrophage function in newborn lambs. *J. Appl. Physiol.* **73**, 2608-2615 (1992).
- 13 Csukás, D., Urbanics, R., Wéber, G., Rosivall, L. & Szebeni, J. Pulmonary intravascular macrophages: prime suspects as cellular mediators of porcine CARPA. *Eur. J. Nanomed.* **7**, 27-36 (2015).
- 14 Zhang, X. *et al.* Regulation of Toll-like receptor-mediated inflammatory response by complement in vivo. *Blood* **110**, 228-236 (2007).
- 15 Moghimi, S. M. Complement propriety and conspiracy in nanomedicine: perspective and a hypothesis. *Nucleic Acid Ther.* doi:10.1089/nat.2015.0587(2016).
- 16 Keyes, J. W., Jr., Wilson, G. A. & Quinonest, J. D. An evaluation of lung uptake of colloid during liver imaging. *J. Nucl. Med.* **14**, 687-691 (1973).
- 17 Imarisio, J. J. Liver scan showing intense lung uptake in neoplasia and infection. *J. Nucl. Med.* **16**, 188-190 (1975).
- 18 Moghimi, S. M. *et al.* Complement activation cascade triggered by PEG-PL engineered nanomedicines and carbon nanotubes: the challenges ahead. *J. Control. Release* **146**, 175-181, (2010).
- 19 Chanan-Khan, A. *et al.* Complement activation following first exposure to pegylated liposomal doxorubicin (Doxil): possible role in hypersensitivity reactions. *Ann. Oncol.* **14**, 1430-1437 (2003).
- 20 Szebeni, J. *et al.* Liposome-induced complement activation and related cardiopulmonary distress in pigs: factors promoting reactogenicity of Doxil and AmBisome. *Nanomedicine* **8**, 176-184 (2012).
- 21 Moghimi, S. M., Hamad, I., Andresen, T. L., Jorgensen, K. & Szebeni, J. Methylation of the phosphate oxygen moiety of phospholipid-methoxy(polyethylene glycol)

- conjugate prevents PEGylated liposome-mediated complement activation and anaphylatoxin production. *FASEB J.* **20**, 2591-2593 (2006).
- 22 Andersen, A. J. *et al.* Single-walled carbon nanotube surface control of complement recognition and activation. *ACS Nano* **7**, 1108-1119 (2013).
- 23 Moghimi, S. M. & Murray, J. C. Poloxamer-188 revisited: a potentially valuable immune modulator? *J. Natl. Cancer Inst.* **88**, 766-768 (1996).
- 24 Laverman, P., Carstens, M. G., Storm, G. & Moghimi, S. M. Recognition and clearance of methoxypoly(ethyleneglycol)2000-grafted liposomes by macrophages with enhanced phagocytic capacity. Implications in experimental and clinical oncology. *Biochim. Biophys. Acta* **1526**, 227-229 (2001).
- 25 Kolhar, P. *et al.* Using shape effects to target antibody-coated nanoparticles to lung and brain endothelium. *Proc. Natl. Acad. Sci. USA* **110**, 10753-10758, (2013).
- 26 Lu, Z. S., Qiao, Y., Zheng, X. T., Chan-Park, M. B. & Li, C. M. Effect of particle shape on phagocytosis of CdTe quantum dot-cystine composites. *MedChemComm* **1**, 84-86 (2010).
- 27 Champion, J. A. & Mitragotri, S. Role of target geometry in phagocytosis. *Proc. Natl. Acad. Sci. USA* **103**, 4930-4934 (2006).
- 28 Geng, Y. *et al.* Shape effects of filaments versus spherical particles in flow and drug delivery. *Nat. Nanotechnol.* **2**, 249-255 (2007).
- 29 Chambers, E. & Mitragotri, S. Prolonged circulation of large polymeric nanoparticles by non-covalent adsorption on erythrocytes. *J. Control. Release* **100**, 111-119 (2004).
- 30 Anselmo, A. C. *et al.* Delivering nanoparticles to lungs while avoiding liver and spleen through adsorption on red blood cells. *ACS Nano* **7**, 11129-11137 (2013).
- 31 Jansen, J. H., Hogasen, K. & Mollnes, T. E. Extensive complement activation in hereditary porcine membranoproliferative glomerulonephritis type II (porcine dense deposit disease). *Am. J. Pathol.* **143**, 1356-1365 (1993).
- 32 Wibroe, P. P., Ahmadvand, D., Oghabian, M. A., Yaghmur, A. & Moghimi, S. M. An integrated assessment of morphology, size, and complement activation of the PEGylated liposomal doxorubicin products Doxil[®], Caelyx[®], DOXOrubicin, and SinaDoxosome. *J. Control. Release* **221**, 1-8 (2016).
- 33 Hamad, I. *et al.* Distinct polymer architecture mediates switching of complement activation pathways at the nanosphere-serum interface: implications for stealth nanoparticle engineering. *ACS Nano* **4**, 6629-6638 (2010).
- 34 Montalescot, G. *et al.* Evaluation of thromboxane production and complement activation during myocardial ischemia in patients with angina pectoris. *Circulation* **84**, 2054-2062 (1991).
- 35 Gaca, J. G. *et al.* Prevention of acute lung injury in swine: depletion of pulmonary intravascular macrophages using liposomal clodronate. *J. Surg. Res.* **112**, 19-25 (2003).
- 36 Moghimi, S. M., Hunter, A. C. & Andresen, T. L. Factors controlling nanoparticle pharmacokinetics: an integrated analysis and perspective. *Annu. Rev. Pharmacol. Toxicol.* **52**, 481-503 (2012).
- 37 Decuzzi, P. *et al.* Size and shape effects in the biodistribution of intravascularly injected particles. *J. Control. Release* **141**, 320-327 (2010).
- 38 Decuzzi, P., Lee, S., Bhushan, B. & Ferrari, M. A theoretical model for the margination of particles with blood vessels. *Ann. Biomed. Eng.* **33**, 179-190 (2005).
- 39 Castells, M. Desensitization for drug allergy. *Curr. Opin. Allergy Clin. Immunol.* **6**, 476-481 (2006).
- 40 Bugna, S. *et al.* Surprising lack of liposome-induced complement activation by artificial 1,3-diamidophospholipids in vitro. *Nanomedicine* **12**, 845-849 (2016).
- 41 Moghimi, S. M. Recent developments in polymeric nanoparticle engineering and their applications in experimental and clinical oncology. *Anti-Cancer Agent. Med. Chem.* **6**, 553-561 (2006).
- 42 Szebeni, J. *et al.* Hemodynamic changes induced by liposomes and liposome-encapsulated hemoglobin in pigs: a model of pseudollargic cardiopulmonary reactions

- to liposomes. Role of complement and inhibition by soluble CR1 and anti-C5a antibody. *Circulation* **99**, 2302-2309 (1999).
- 43 Meszaros, T. et al. Factor H inhibits complement activation induced by liposomal and
micellar drugs and the therapeutic antibody rituximab in vitro. *Nanomedicine*
doi:10.1016/j.nano.2015.11.019 (2016).
- 44 Wu, Y. Q. et al. Protection of nonself surfaces from complement attack by factor H-
binding peptides: implications for therapeutic medicine. *J. Immunol.* **186**, 4269-4277
(2011).
- 45 Rodriguez, P. L. et al. Minimal “self” peptides that inhibit phagocytic clearance and
enhance delivery of nanoparticles. *Science* **339**, 971-975 (2013).
- 46 Perry, J. L., Herlihy, K. P., Napier, M. E. & Desimone, J. M. PRINT: a novel platform
toward shape and size specific nanoparticle theranostics. *Acc. Chem. Res.* **44**, 990-998
(2011).
- 47 Mollnes, T. E. et al. Essential role of the C5a receptor in E-coli-induced oxidative burst
and phagocytosis revealed by a novel lepirudin-based human whole blood model of
inflammation. *Blood* **100**, 1869-1877 (2002).
- 48 Bergseth, G. et al. An international serum standard for application in assays to detect
human complement activation products. *Mol. Immunol.* **56**, 232-239 (2013).

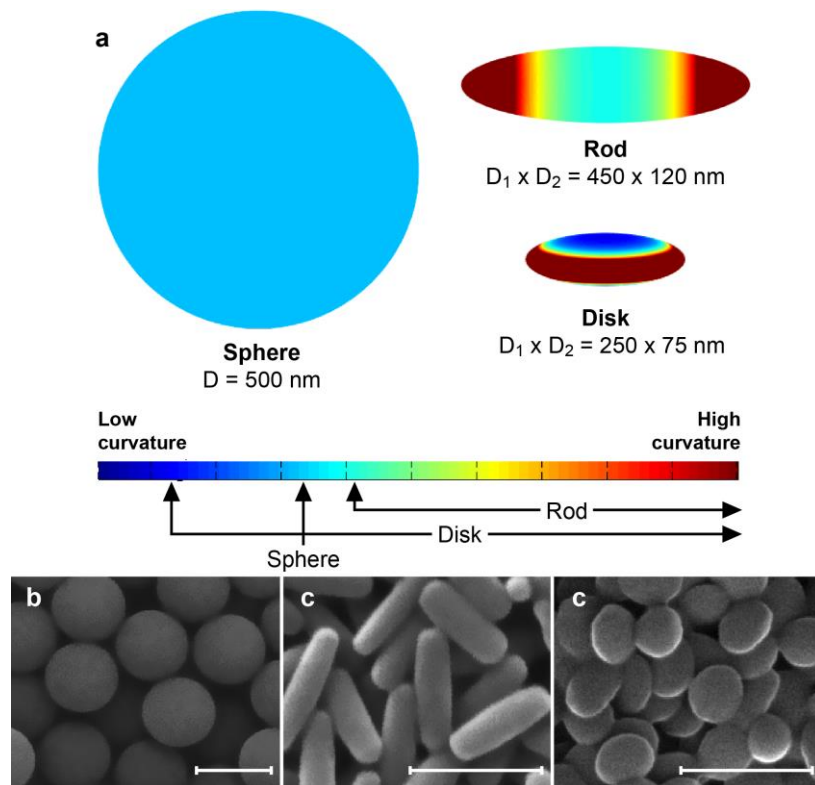


Figure 1. Graphical and scanning electron microscopy (SEM) representation of spheres, rods, and disks. **a:** True relative size and shape with colours representing Gaussian curvature (assuming rods and disks as prolate and oblate spheroids, respectively). **b-d:** SEM images of spheres (b), rods (c) and disks (d). Scale bars: 500 nm.

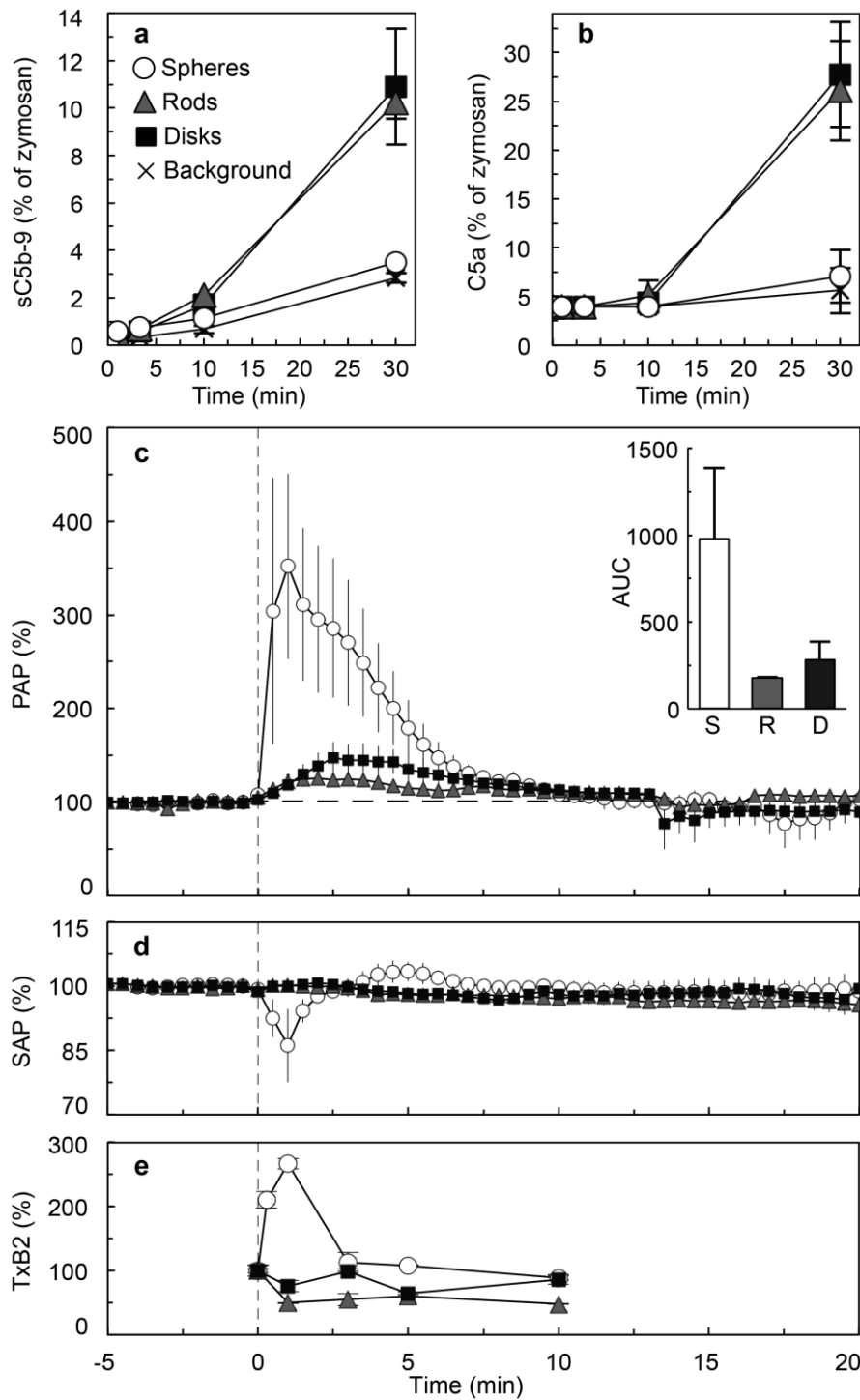


Figure 2. Changes in complement activation in pig blood and pig haemodynamic parameters after exposure to spheres (circles), rods (triangles) and disks (squares). **a & b:** Time-dependent complement activation in pig whole blood shown as percentage of formed sC5b-9 and C5a, respectively, relative to a 0.2 mg/mL zymosan response. Values are given as mean \pm s.d., $n=3$ (sC5b-9: $p<0.01$ for spheres and disks at 10 and 30 min, and $p<0.001$ for rods at 10 and 30 min compared with control/background level). Complement activation by particles was compared on an equivalent surface area of $\sim 14,500$ mm²/mL of blood. Absolute values of complement activation products are presented in **Supplementary Figure S1**. **c:** Time-dependent changes in pulmonary arterial pressure (PAP) on particle injection. Particles (given on an equivalent surface

area of $\sim 114,300 \text{ mm}^2/20 \text{ kg}$ body weight) were injected at zero time. Inset: Integrated area under the curve (AUC) of the changes in PAP during the first 10 min of injection. **d:** Changes in the systemic arterial pressure (SAP) on particle injection. **e:** Changes in levels of thromboxane B2 (TxB2) on particle injection. The results from pig experiments are expressed as mean \pm s.e.m. of injections (n=3).

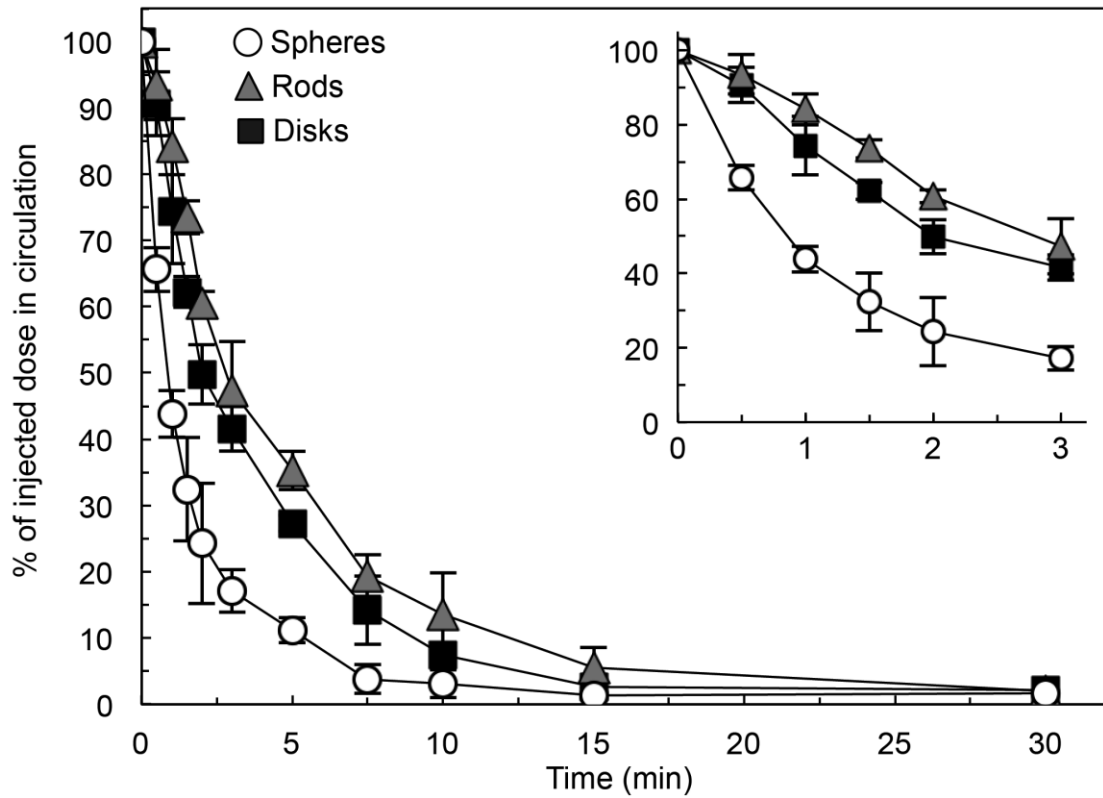


Figure 3. Circulation profile of spheres, rods and disks following intravenous injection into pigs. Spheres are cleared faster compared to rods and disks. The inset is a magnified representation of early time points. The results are expressed as mean \pm s.e.m (n=3).

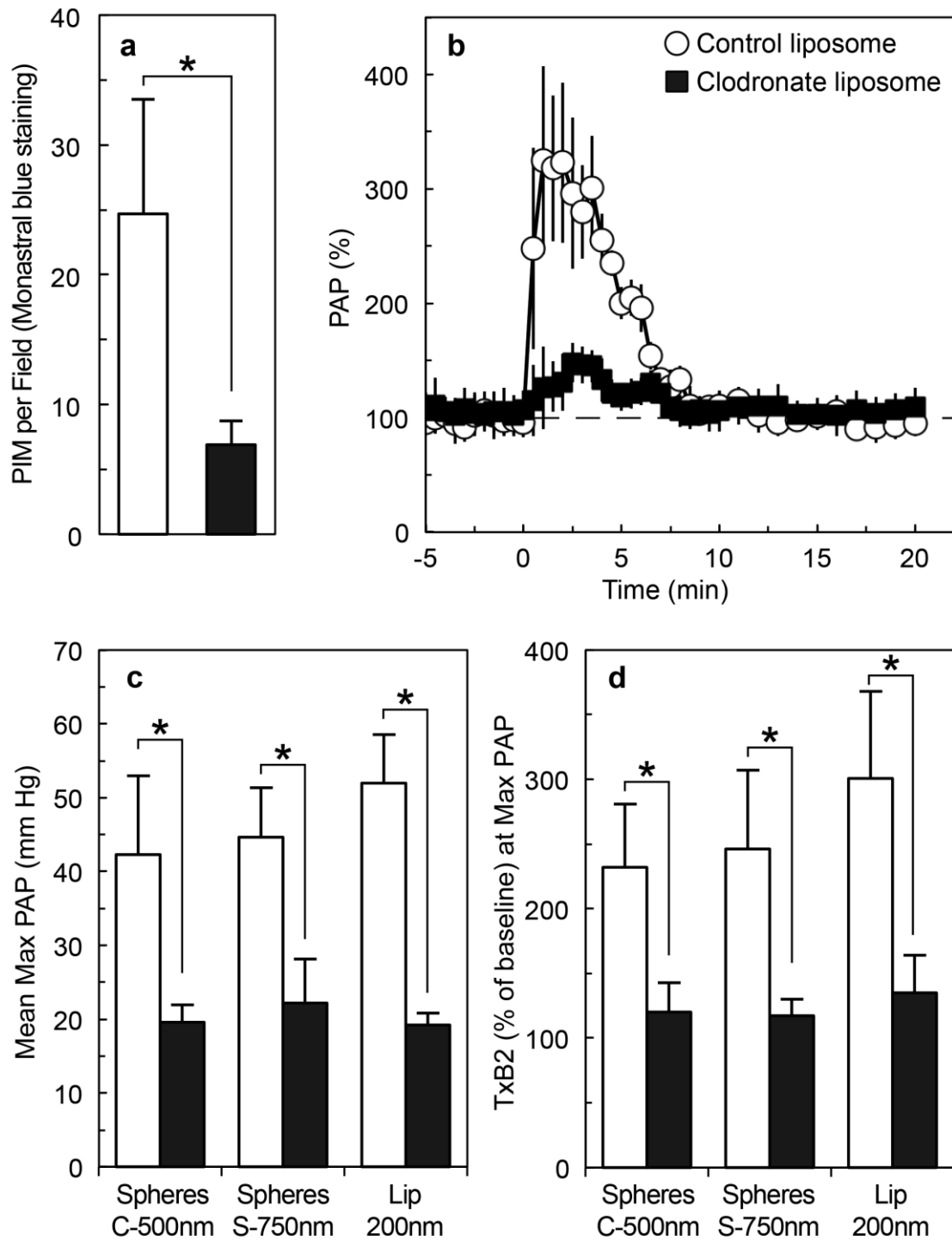


Figure 4. Dampening of particle-mediated haemodynamic changes in pigs following pulmonary intravascular macrophage (PIM) depletion. **a:** number of positive PIM cells per high-powered field in lung samples untreated and clodronate-liposome-treated pigs (the results represents 15 random biopsy lung specimens per animal \pm s.e.m.; n=2 pigs per group). **b:** Time-dependent changes in pulmonary arterial pressure (PAP) in control and clodronate-liposome-treated pigs. Animals were injected intravenously with spherical carboxylated polystyrene particles of 500 nm (1.5×10^{11} particle/20 kg body weight) at zero time. **c:** Comparison of maximum PAP in control and clodronate-liposome-treated pigs on intravenous injection of 500 nm

carboxylated polystyrene particles (C-500nm), 750 nm sulfated polystyrene particles (S-750nm) and 200 nm PEGylated liposomes (Lip 200nm). Polystyrene particles were injected at a dose of 1.5×10^{11} particle/20 kg body weight and liposomes at a dose of 10 mg total lipid/20 kg body weight. **d**: Changes in levels of thromboxane B2 (TxB2) on particle injection in control and clodronate-liposome-treated pigs. The results in **b, c & d** are mean \pm s.e.m. (n=2 pigs per group). Open circles and columns represent animals pre-treated with control liposomes and black squares and columns represent pigs pre-treated with clodronate-encapsulated liposomes, respectively. * $p < 0.05$.

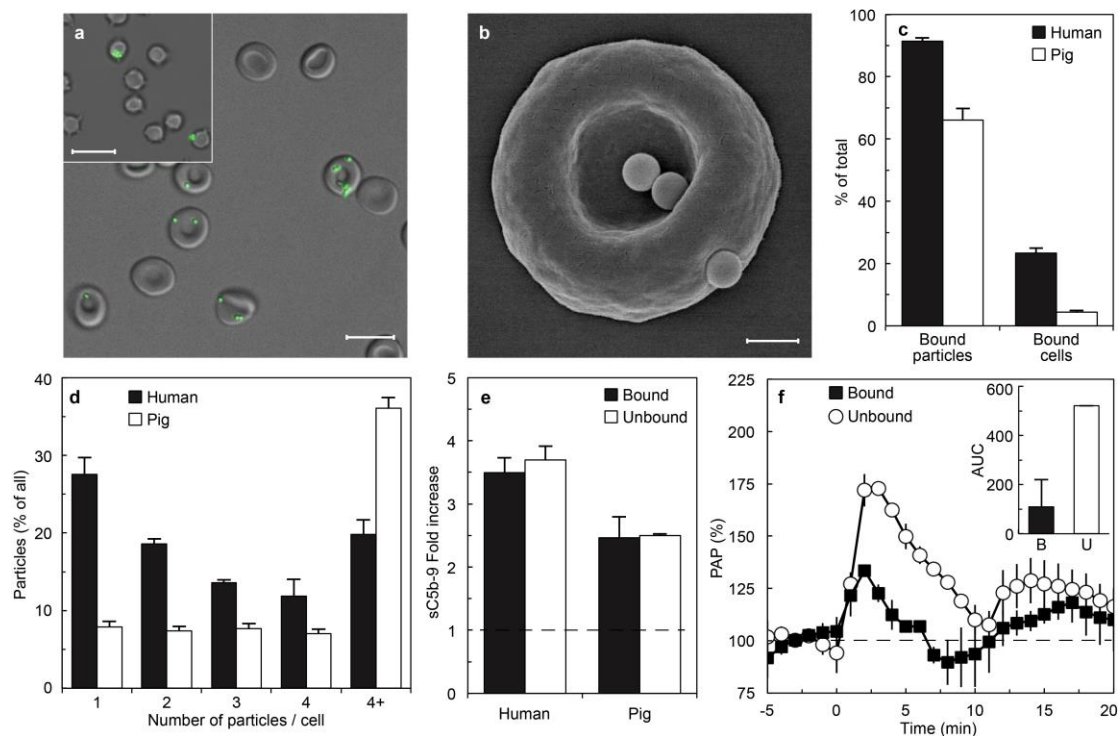


Figure 5. Overcoming adverse reactions to spheres through erythrocyte ‘hitch-hiking’. **a:** DIC/fluorescence images of adhered 750 nm carboxylated polystyrene particles to human and pig (inset) erythrocytes. Scale bars: 10 μm . **b:** SEM image of a human erythrocyte with adhered polystyrene particles. Scale bar: 1 μm . **c&d:** Quantitative assessment of the particle-cell interaction by FACS, showing the fraction of bound particles and cells for human and pig (c) and how particles are distributed on cells (d). Values are expressed as mean \pm s.e.m. of four human donors, each in biological duplicates, and one pig donor in biological triplicates. **e:** Complement responses (sC5b-9 measurements) to erythrocyte-bound and unbound particles in human and pig whole blood. In **c**, **d** & **e** the ratio of human and pig erythrocytes to particles was 2:1 corresponding to 1.13×10^9 and 1.69×10^9 spheres/incubation, respectively. Values are expressed as mean \pm s.d. (see methods for statistical details). **f:** Haemodynamic changes in pigs measured by changes in pulmonary arterial pressure (PAP). Total number of particles injected in both cases was $8.6 \times 10^9/20$ kg body weight. Inset: Area under the curve (AUC) for particles that are bound (B) to erythrocytes or unbound (U). Values are expressed as mean \pm s.e.m. for two pigs.